A ROBOTIC METHOD TO INSERT BATT INSULATION INTO LIGHT-FRAME WOOD WALL FOR PANEL PREFABRICATIONS

Xiao Han, Cheng-Hsuan Yang & Yuxiang Chen
Department of Civil and Environmental Engineering, University of Alberta, Edmonton, Canada

Alejandra Hernandez Sanchez
Institute of Advanced Materials for the Sustainable Manufacturing, Tecnológico de Monterrey, Ciudad de Mexico, Mexico

ABSTRACT: *Currently, industrial robot arms are trending in prefabricated building construction; however, a notable gap exists in established automated processes and related research specifically for the insertion of batt thermal insulation. The current method for accomplishing this task relies on manual insertion, which is labour-intensive for the workers and poses long-term health and safety concerns. This research presents an ongoing research project aimed at developing a feasible robotic process for the automated insertion of batt thermal insulation into prefabricated light-frame wood wall frames. This research focuses on the utilization of a single 6-degree-of-freedom robot arm for the insertion process, complimented by the design of a custom-built end-effector. The proposed robotic insertion process, named GLITPP, comprises of six major steps: (1) Grasp, (2) Lift, (3) Insert, (4) Tilt, (5) Push, and (6) Press. The GLITPP insertion process, along with the custom-built end-effector effectively mitigates the influence of the insulation's nonlinear mechanical properties, while also taking collision avoidance into consideration. This ensures a tight-fitting insulation within the frame cavity, without visible gaps and deficiencies. The necessary physical operating parameters for the insertion process, such as angles, offset, and force requirements, are identified to ensure the precision, efficiency, and repeatability of insertion. A prototype of the designed end-effector is used to demonstrate and validate the robotic method, achieved a high success rate of 93.3%. The development of this research will further advance the complete automation of light-frame wood wall panel prefabrication, offering the industry a wider range of options for selecting thermal insulation for their processes.*

KEYWORDS: *Robotic Building Prefabrication; Robotic Insertion; Light-frame Wood Construction; Robotic End-effector; Automation in Construction; Thermal Insulation*

1. INTRODUCTION

Industrial robot arm technology is increasingly being demonstrated and utilized in building construction processes due to its cost effectiveness, ease of programmability, high accuracy, and capacity (Chai et al., 2022; Koerner-Al-Rawi, Park, Phillips, Pickoff, & Tortorici, 2020; Leung, Apolinarska, Tanadini, Gramazio, & Kohler, 2021). Robot arms support mass production due to their high efficiency in performing repetitive tasks and their scalability, making them particularly suitable for the construction of prefabricated modular light-frame wood wall panels. These panels are prefabricated offsite, incorporating essential building elements such as framing, insulation, and sheathing. The use of robotic arms for cutting, assembling, and nailing timber for framing and sheathing is already well established and utilized (Stricot-Tarboton, 2019).

Various insulating materials are available on the market for timber framed structures, but the common types include blow-in insulation, spray foam insulation, and batt thermal insulation, made from fiberglass or mineral wool. Among these, batt thermal insulation holds a dominant market position due to their low cost to effective thermal performance ratio (Latif, Bevan, & Woolley, 2019). Currently, the automated insulation installation solution used to support the construction of modular light-frame wood wall panels are blow-in insulation (Orlowski, 2020) and spray-foam ("SprayWorks Equipment" n.d.; "Spray-R" n.d.), due to their loose form and ability to easily conform to voids. However, batt thermal insulation still needs to be manually installed by workers in the light-frame wood wall panel construction process (Stricot-Tarboton, 2019), which hinders achieving a fully automated construction process using this type of insulation.

The mechanical behaviors of batt insulation made of either mineral wool or fiberglass are classified as semi-rigid and non-rigid, respectively. In terms of mechanical properties, both these insulations are considered anisotropic deformable materials due to random fiber orientation. The result is that the rigid body assumption cannot be employed. In addition, predicting deformation and deflection of insulation using classical approaches is insufficient. Furthermore, the relationship between stress and strain is nonlinear thus complicating the modelling

Referee List (DOI: 10.36253/fup_referee_list)
FUP Best Practice in Scholarly Publishing (DOI 10.36253/fup_best_practice)
Xiao Han, Cheng-Hsuan Yang, Yuxiang Chen, Alejandra Hernandez Sanchez, *A Robotic Method to Insert Batt Insulation into Light-Frame Wood Wall for Panel Prefabrications,* pp. 594-604, DOI 10.36253/979-12-215-0289-3.58

process which has downstream effects on simulation and analysis. To the best of our knowledge, there has been no formal study or research on the robotic process of inserting anisotropic deformable material into a shallow cavity for a tight-fit. Manipulating deformable objects presents challenges as classical analytical force relationships are no longer applicable. Consequently, predicting and controlling material behavior during manipulation requires complex contact analysis and modeling of nonlinear material behavior (Arriola-Rios et al., 2020; Zaidi, Corrales, Bouzgarrou, Mezouar, & Sabourin, 2017).

The successful development of this research will allow for direct integration into existing prefabricated modular light-frame wood wall panels construction processes to realize full automation or prefabricated construction using batt thermal insulation. The implementation of this automated process offers several benefits, including the elimination of risks to workers from developing chronic respiratory diseases due to exposure to airborne dust and fibers, as well as reducing their exposure to carcinogens and volatile organic compounds. Additionally, it will decrease the ergonomic risk arising from repetitive movements during manual insulation installation. (BREUM, SCHNEIDER, JØRGENSEN, VALDBJØRN RASMUSSEN, & SKIBSTRUP ERIKSEN, 2003; Kupczewska-Dobecka, Konieczko, & Czerczak, 2020; Li, Han, Gül, & Al-Hussein, 2019).

This paper is structured into six sections. Section 2 introduces the research objectives. In section 3, the design concept of the robotic end-effector and robotic insertion process are explained. Section 4 covers the implementation and parameters identification. Following that, Section 5 presents the outcomes of the conducted experiments, providing an in-depth analysis of the results. Lastly, Section 6 presents our conclusions and outlines potential avenues for future research and development.

2. RESEARCH OBJECTIVES

This research aims to develop a robotic method to automatically insert batt thermal insulation into a light-frame wood wall frame. Studies have been conducted to explore the process of utilizing industrial robot arms to insulate wall panels through blow-in insulation and spray foam insulation methods. However, the utilization of robotic methods for inserting batt insulation has been rarely discussed. When implementing the robot arm for batt insulation insertion, the most critical challenges are effectively manipulating deformable materials, along with ensuring collision-free trajectories for the robot arm. To achieve the goal of automatically inserting batt thermal insulation using robotic methods, the objectives of this research will focus on the following:

1. Designing a robotic end-effector capable of proficiently manipulating batt thermal insulation, while considering its geometrical properties and deformable material behaviors.
2. Developing a robotic process for inserting batt thermal insulation into light-frame cavities using the proposed robotic end-effector to mitigate the influence of the deformation uncertainties and nonlinear mechanical properties.
3. Identifying variable parameters (e.g., angles, location, forces, etc.) of the developed robotic process to ensure the integrity and success of insertion and to minimize potential collisions.

3. ROBOTIC END-EFFECTOR & INSERTION PROCESS DESIGN

The developed robotic method contains two major parts: the robotic end-effector and the robotic insertion process. First, to facilitate the pickup and manipulate batt insulation to correct positions, a dedicated robotic end-effector was designed. Then, a robotic insertion process with six major steps was developed to effectively insert the batt insulation into the light-frame.

3.1 Assumptions

The developed robotic insertion process is based on the following three assumptions:

1. The light-frame wood wall is a typical straight wall without any piping or wires within the cavity.
2. The wood stud utilized in the frame is in a favorable condition, with negligible warping.
3. The working platform features a smooth surface, and the friction between the insulation and the working platform is considered negligible.

3.2 Robotic End-effector Design

Illustrated in Figure 1, the end-effector comprises four components: a two-finger gripper, a force-torque sensor, an adaptor, and a pair of gripping jaws. The two-finger gripper with linear stroke is an off-the-shelf product. For standard batt insulation, its width is larger than the width of the cavity to achieve a tight-fit once inserted. These dimensional differences require the robot arm to apply compressive force to insert the batt insulation into the cavity. Therefore, a force-torque sensor that allows control of the applied force is mounted atop of the two-finger gripper. The gripping jaw adaptors are designed to connect the off-the-shelf gripper to the gripping jaws. The adaptors are CNC-machined L-shaped steel braces. The last component of the end-effector is the custom-built gripping jaws. The surface inside the jaw is textured to increase friction, with all else being equal reduces the grasping force, between the jaw and the insulation. The sizing of the jaw should be determined considering the dimensions and weight of the insulation, as well as its degree of elasticity. The jaw dimension is crucial to minimize the permanent deformation during manipulation.

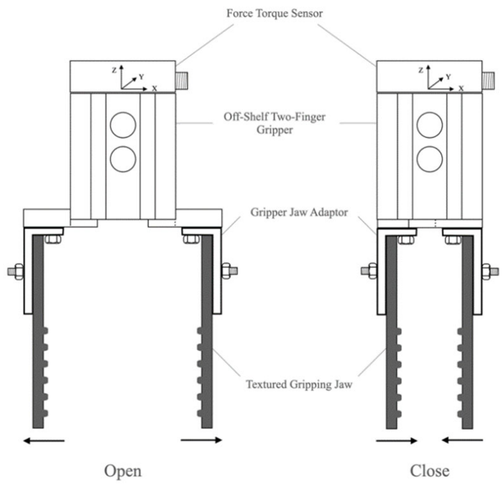

Figure 1. The proposed robotic end-effector.

3.3 Robotic Insertion Process Design

The proposed process for inserting batt insulation in this section is inspired by both the manual insertion process and the research conducted by Kim & Seo (2019). The research focused on the insertion of rigid objects into shallow cavities, incorporating primitive operations such as grasping, tilting, and tucking. In the context of batt insulation insertion, the proposed robotic insertion process, coined as GLITPP, contains six major steps: (1) Grasp, (2) Lift, (3) Insert, (4) Tilt, (5) Push, and (6) Press (as illustrated in Figure 2).

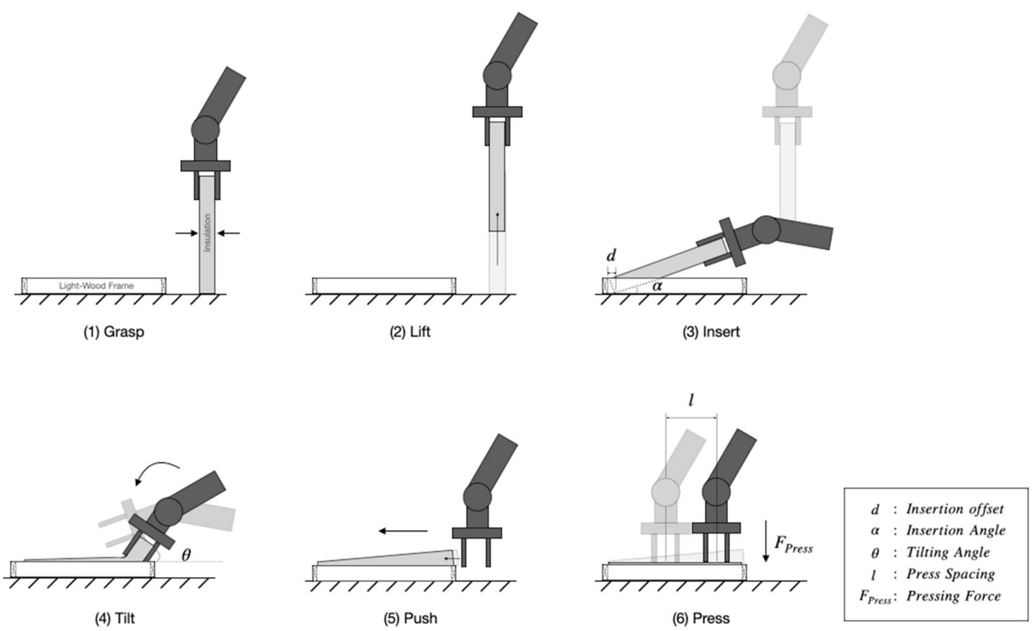

Figure 2. The GLITPP insertion process.

The initial step is to grasp the insulation from an initialized position. The robot arm moves to the top of the insulation using a point-to-point motion (PTP motion). Subsequently, the robot arm descends linearly (LIN motion) until the gripper reaches the insulation's top edge. Upon reaching the edge, the gripper closes to securely grasp the insulation. The second step is lifting. After grasping the insulation, a LIN motion is utilized to lift the insulation linearly. This is followed by a PTP motion to position the insulation in proximity of the frame cavity. In the third step, a combination of PTP and LIN motions is programmed to insert one edge of the insulation into the frame cavity with consideration of an insertion angle (α) and offset (d). For the fourth step, the end-effector is tilted. This ensures that when the grippers open, they avoid collisions with the frame and release the insulation without shearing it. Achieving this involves a PTP motion, tilting the end-effector to a specific angle (θ), and then releasing the insulation. To align the insulation accurately with the frame, pushing operations are employed along the uninserted edges. The robot arm utilizes LIN motions to enable the gripping jaws to gently push the insulation until it aligns flush with the cavity. For the final step, the gripping jaws are employed to press the uninserted edges of the insulation into the frame cavity, using defined press spacing (l) and pressing force (F_{Press}) parameters. The pressing pattern initiates from the corners of the inserted edge and proceeds along the edges perpendicular to the inserted edge and then finally along the parallel uninserted edge. The task description and associated robot motions outlined above are summarized in Table 1.

Table 1. Six steps of the GLITPP insertion process.

Steps	Task Description	Related robot motions
Grasp	From the initial position, the insulation is securely grasped by robotic gripper for pick up and manipulating.	1. PTP motion to the top of the insulation. 2. LIN motion down till the gripper reaches the insulation's edge. 3. Close the gripper.
Lift	The robot arm picks up the insulation and moves it close to the frame cavity.	1. LIN motion to lift the insulation. 2. PTP motion to move the insulation close the frame cavity.
Insert	The robot arm inserts the insulation into the cavity with an insertion angle (α) and offset (d).	1. PTP motion to rotate the insulation. 2. LIN motion to insert the insulation into the cavity.
Tilt	The robot arm tilts the insulation to a tilting angle (θ).	1. PTP motion to tilt the insulation
Push	The robot arm uses its gripping jaw to push the insulation along the uninserted edges of the insulation until it is flushed with the cavity.	1. LIN motion down till tip of the gripping jaw reaches the bottom of the insulation. 2. LIN motions parallel to the frame's direction to push the insulation into the cavity.
Press	The robot arm uses its gripping jaws to press the insulation into the frame cavity.	1. PTP motion to the pressing location. 2. LIN motions descend till the force reaches the pressing force. 3. LIN motion up. 4. LIN motion to the section pressing location 5. Repeat step 2 to 4 until the insulation is inserted.

4. IMPLEMENTATION & PARAMETER INDETIFICATIONS

4.1 Prototype of the End-effector

For the implementation, this research developed a prototype of the robotic end-effector (Figure 3). Detailed specifications of the end-effector components are listed in Table 2. The Robotiq FT 300-S Force Torque sensor, capable of measuring forces up to ±300 N and offering a data output of 100 Hz was utilized. Additionally, the Robotiq Hand-e gripper, with a maximum stroke length of 2 inches, was selected to serve as the parallel gripper. The custom adaptor was designed, in accordance with the Hand-e gripper specifications, to incorporate M3 screws for attachment onto the gripper's tracks. The gripping jaws, with dimensions of 4 inches by 4.5 inches and a thickness of 3/16 inch, were 3D printed with a textured interior surface at the lower section. The final assembly of the end-effector provides a clearance of 3.75 inches when the gripper is open and reduces to 1.75 inches when closed.

Figure 3. The prototyped robotic end-effector at Fully open position (left) and at fully closed position (right).

Table 2. Specifications for the prototyped end-effector.

Part	Manufacturer	Model	Specifications
Force torque sensor	Robotiq	FT 300-S	• Measuring range: ±300 N • Data output rate:100 Hz
Two-finger gripper	Robotiq	Hand-e	• Stroke: 2 in • Form-fit grip payload: 11 lbs • Friction grip payload: 8.8 lbs • Weight: 2 lbs • Gripping force: 20 to 185N
Adaptor	Custom-built	-	• Material: CNC machined steel
Gripping jaws	Custom-built	-	• Material: 3D printed PLA • Size: 4-inch (W) × 4.5-inch (L) × 3/16-inch (T)

4.2 In-lab Robotic Cell Setup

The in-lab robotic cell setup is illustrated in Figure 4. A Universal Robot UR5e was utilized as the robotic manipulator. The UR5e is a robot arm with 6 degree-of-freedoms. Its operational capacity is 11 lbs for payloads and accompanied by a maximum reach span of 33.5 inches. The robot arm was mounted on 46 inches by 34 inches table platform. The platform's upper surface is constructed from plastic, providing a smooth texture that minimizes friction effects between the insulation and the surface. Ultimately, the prototyped end-effector was affixed to the 6th axis of UR5e.

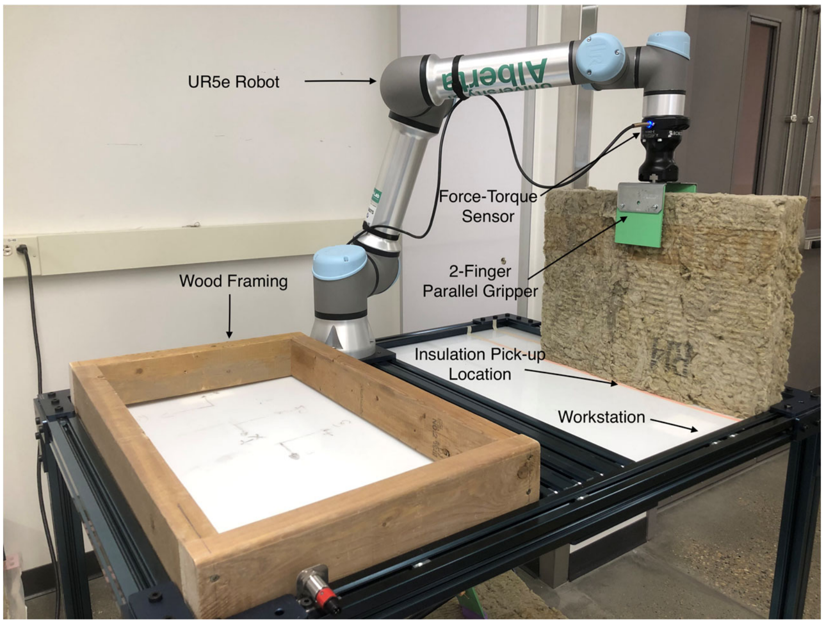

Figure 4. The in-lab robotic cell setup.

The light-frame wood wall utilized in this research is constructed using four 2 inches by 4 inches SPF Dimensional Lumbers. This lumber dimension is representative of a common type of light-frame wood wall used in building construction. The spacing between wood studs is set at 16 inches on-center, a standard stud spacing commonly employed in building construction, which results in a cavity width of 14.5 inches. Due to hardware constraints, specifically the reach of the robotic arm, the height of the wall cavity has been scaled to 26 inches, instead of the typical 8-foot wall. The overall dimensions of the wood cavity are 14.5 inches in width, 26 inches in height, and 3.5 inches in depth.

4.3 Parameters Identification

The GLITPP insertion process involves five key parameters: insertion angle (α), insertion offset (d), tilt angle (θ), press spacing (l) and pressing force (F_{Press}). These parameter values are determined through a series of individual robotic trials. All the trials are tested on 26 inches of mineral wool insulation. Once a set of feasible parameter values are ascertained, they are integrated to illustrate and formalize the entire robotic insertion process, the results of which will be presented in Section 5.

4.3.1 Insertion angle & Insertion offset & Tilt angle

There exists an interdependency among the insertion angle (α), insertion offset (d), and tilt angle (θ). Changes in the values of one parameter affect the other, as demonstrated by Eq.1. This equation represents an affine function that defines all points (x, y) on the outer surface of the fully opened gripper jaw in its tilted position. Notably, the parameter values must satisfy the condition that the affine function (hyperplane) is positioned to the left of the boundary point (P). This arrangement ensures collisions-free between the frame and the gripper. Figure 5 illustrates the variables used in Eq.1: L represents the distance from the tool center point (TCP) to the end of the insulation, H is the wood stud width, which is equal to the insulation thickness, W denotes the frame cavity width, E stands for the distance from the TCP to end of the gripper, G represents the distance between the center line and the outer surface of the gripper jaw in its fully open position, and P corresponds to the inner edge of the wood stud, serving as the boundary point.

$$y = (2x * \sin(\theta) - 2L * \sin(\theta - \alpha) + H * \cos(\theta - \alpha) - 2 * d * \sin(\theta) - 2G)/(2\cos(\theta)) \tag{1}$$

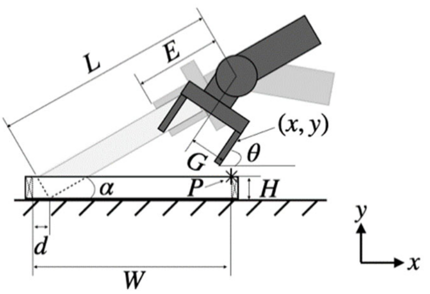

Figure 5. Illustration of the variables in Eq.1.

Due to the texturing on the gripper, a tilt operation is employed to facilitate the release of insulation from the gripper jaws after insertion into the frame cavity. This approach reduces disruptions to the insulation's intended position, prevents damage to its fibers by eliminating shearing, and allows for maintaining a minimal insertion angle. Thus, obtaining the minimum tilt angle is essential for achieving the effective release of insulation. The determination of this minimum tilt angle then allows for the calculation of the insertion angle and offset. Moreover, tilting indirectly contributes to the insertion process by pressing more edges of the insulation into the frame cavity. The minimum tilt angle is determined to be 55°, factoring in the insulation's weight and frictional forces. A list of trialed tilt angles and their corresponding outcomes are presented in Table 3.

Table 3. A list of trialed tilt angles with success rate.

θ (°)	Success Rate	Failure Mode
30	0/5	Insulations were pulled out of the frame cavity.
45	0/5	Insulations were first pulled, followed by shearing of the insulation fibers.
55	5/5	N/A

The insertion offset is the distance between the insulation and the frame's edge. When the offset is either too small or too large, the risk of collision increases during the insertion or pressing steps, respectively. This necessitates finding a balance between within the feasible range of offsets. Regarding the insertion angle, a smaller angle results in a longer edge of the insulation being inserted into the frame cavity. This minimizes the likelihood for the insulation edges to catch or snag during the subsequent titling and pressing steps, thus, ensuring proper seating of the insulation within the frame cavity. The lower limit of the insertion angle depends on the tilt angle in order to prevent collisions after titling when the grippers open to release the insulation. The insertion angle for a specific insertion offset, utilizing the minimum tilt angle obtained earlier, can be determined from Figure 6. This figure is generated by computing the solution pairs that satisfy Eq.1. Three combinations were selected for testing and the results are presented in Table 4. The tested minimum feasible combination of insertion angle and insertion offset is achieved at 30° with an offset of 0.75 inches.

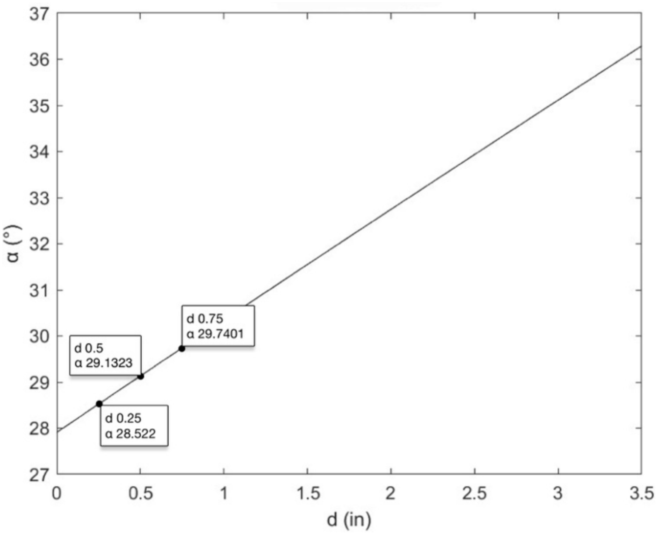

Figure 6. Combination of insertion angle and insertion offset.

Table 4. A list of trialed combination of insertion angle and insertion offset with success rate.

α (°)	d (in)	Success Rate	Failure Mode
29	0.25	0/5	Collision warning during insertion due to excessive compression of insulation.
29.5	0.5	0/5	Collision warning during insertion due to excessive compression of insulation.
30	0.75	5/5	N/A

4.3.2 Press spacing

The press spacing signifies the positions where the gripper will apply pressure along the uninserted edge of the insulation, facilitating its complete insertion into the frame cavity while ensuring no insulation edges remain exposed. While there are no explicit limitations on the quantity of presses, minimizing press count contributes to time efficiency. In the conducted trials, the center-to-center distance of the press spacing varies from 15 inches to 5 inches, with the initial press initiated from a corner. The outcomes of the trials are compiled in Table 5. It was noted that a 5-inch press spacing effectively accomplishes the insulation's insertion into the frame cavity, without any conspicuous convexity.

Table 5. A list of trialed press spacing with success rate.

l (in)	Success Rate	Failure Mode
15	0/5	Evident convexity noticeable between each press point.
10	3/5	Evident convexity noticeable between certain press points.
5	5/5	N/A

4.3.3 Pressing force

Once the press spacing is determined, it becomes crucial to apply the minimum amount of force necessary to press the insulation into the frame cavity. This approach ensures that the insulation avoids permanent deformation, which could lead to a loss of effective R-value. The lower and upper bounds for the pressing force are 80N and 120N, respectively. The results of the trials are listed in Table 6. It was determined that a pressing force of 100N fully and reliably presses the insulation into the frame cavity each time.

Table 6. A list of trialed pressing force with success rate.

F_{Press} (N)	Success Rate	Failure Mode
80	2/5	There were instances that the insulation was not fully pressed in.
100	5/5	N/A
120	4/5	There was an instance where the insulation had permanent deformation.

5. VALIDATION

The designed GLITPP insertion process, using the parameters obtained above as shown in Table 7, was tested with mineral wool and fiberglass batt insulations in two distinct scenarios that represent the actual configurations of insulation installation in construction: (1) a single piece of insulation filing the entire frame cavity, and (2) two pieces of insulation planed in tandem within the frame cavity. In Scenario 2, the process involved two steps: first inserting the 20-inch piece and then 6-inch piece to fill the entire frame cavity. During the insertion of the 6-inch piece, an additional 1-inch offset was applied between the two insulations to avoid the interaction of large frictional forces between the mating surfaces. For Scenario 1, ten tests were conducted for each insulation type. For Scenario 2, ten tests were conducted for each step and each insulation type. Each test was performed using new insulation to simulate the actual application in construction.

Table 7. Summarized selected parameter values obtained from Section 4.3.

Parameter	Value
Tilt Angle (θ)	55°
Insertion Angle (α)	30°
Insertion Offset (d)	0.75 in
Press Spacing (l)	5 in
Pressing Force (F_{Press})	100 N

5.1 Results and Discussion

Table 8 summarizes the experiment results using the selected parameters obtained in Section 4.3. Fig. 8 shows the progress of all the experiments and final insertion completion with the front and back of the insulation. The success of the entire GLITPP insertion process is defined by the insulation fitting tightly within the frame cavity, the absence of visible voids and gaps between the insulation and wood frame, and the insulation having no shearing or permanent deformation. The overall success rate stands at 93.3%.

Table 8. Experiment results for entire GLITPP insertion process.

Scenario	Insulation Length (in)	Batt Insulation Type	Success Rate
1	26	Mineral Wool	9/10
1	26	Fiberglass	10/10
2.1	20	Mineral Wool	10/10
2.1	20	Fiberglass	9/10
2.2	6	Mineral Wool	8/10
2.2	6	Fiberglass	10/10

Figure 8. Experiment progress. Each row is the scenario associated with the corresponding rows of the Table 7.

The high success rates, as showed in Table 8, were achieved by mitigating the negative effects of deformation and uncertainties in mechanical properties through the GLITPP insertion process. The integration of individual parameter identification into a single continuous process, facilitated by custom-built grippers, is seamless and repeatable. The results substantiate that the manipulation of deformable insulation using the designed grasping, lifting, and inserting steps yields high accuracy in achieving target positions. The tilting step reduces the risk of shearing of the insulation during release, while the pushing step offers guidance that minimizes uncertainties and random disturbances before pressing. Ultimately, the pressing step ensures a tight-fitted insulation within the frame cavity, without any discernible gaps and deficiencies. A notable feature of the GLITPP process is that it can be extended to full-scaled 2x4 light-frame wood wall panels and light-frame wood wall panels with varying wood stud sizes, achieved by employing different sizes/numbers of grippers and tuning of parameters.

There were four instances in which the GLITPP process did not succeed. In scenario 2.1, the failure was an outlier, as no defects were observed in the insulation. For scenarios 1 and 2.2, the lack of success resulted from pre-existing creases and pockets of low-density in the insulation. Notably, the insulations used in validation were all chosen randomly from the packaging without any rejection of unideal pieces of insulation. Incorporating insulation pre-inspection, selection, and rejection would raise the success rate.

6. CONCLUSION

This research introduces a robotic method to insert batt thermal insulation into light-frame wood wall frame. The method comprises two major components: a custom-built end-effector and a corresponding robotic insertion process. The design of the robotic end-effector integrates seamlessly with an off-the-shelf two-finger gripper. The end-effector is constructed of a force-torque sensor, a two-finger gripper, an adaptor, and a pair of gripping jaws. The proposed robotic insertion process, named GLITPP, encompasses a sequence of six major steps: Grasp, Lift, Insert, Tilt, Push, and Press. To identify the variable parameters within the GLITPP insertion process, an in-lab robotic cell equipped with a prototyped end-effector was utilized. Through a series of individual robotic trials and iterative refinements, these parameter values were determined. The effectiveness and feasibility of the proposed robotic method were evaluated using two common batt thermal insulations: mineral wool and fiberglass. Test scenarios encompassed both a single insulation piece filling the entire frame cavity and the tandem placement of two insulation pieces within the cavity. The results exhibited a remarkable 93.3% success rate for the GLITPP insertion process. To ensure the broader applicability of the proposed method, future works will involve testing the GLITPP insertion process on a larger capacity robot arm with full-scaled panels. Additionally, the integration of an insulation condition identifying sensor is envisioned, enhancing adaptability by combining it with our robotic insertion process.

7. ACKNOWLEDGEMENTS

This research was financially supported by Mitacs under Design of Prefabricated Exterior Wall Panels for Robotic Building Retrofit Project ID IT32540, NSERC ALLRP under Practical Methods for Efficient Estimation of Effective Thermal Resistance of Exterior Walls Project ID 566879-21, and Tecnologico de Monterrey under Seed Grant Program Robotic Wall Construction Using Innovative Building Bl and Challenge-Based Research Funding Program 2022 project ID IJXT070-22TE6000.

REFERENCE

Arriola-Rios, V. E., Guler, P., Ficuciello, F., Kragic, D., Siciliano, B., & Wyatt, J. L. (2020). Modeling of Deformable Objects for Robotic Manipulation: A Tutorial and Review. *Frontiers in Robotics and AI*, *7*, 82. https://doi.org/10.3389/frobt.2020.00082

Automated Spray Foam Machines | SprayWorks Equipment. (n.d.). Retrieved July 26, 2023, from https://sprayworksequipment.com/products/spray-robots/spraybot/

BREUM, N. O., SCHNEIDER, T., JØRGENSEN, O., VALDBJØRN RASMUSSEN, T., & SKIBSTRUP ERIKSEN, S. (2003). Cellulosic Building Insulation versus Mineral Wool, Fiberglass or Perlite: Installer's Exposure by Inhalation of Fibers, Dust, Endotoxin and Fire-retardant Additives. *The Annals of Occupational Hygiene*, *47*(8), 653–669. https://doi.org/10.1093/annhyg/meg090

Chai, H., Wagner, H. J., Guo, Z., Qi, Y., Menges, A., & Yuan, P. F. (2022). Computational design and on-site mobile robotic construction of an adaptive reinforcement beam network for cross-laminated timber slab panels. *Automation in Construction*, *142*, 104536. https://doi.org/10.1016/j.autcon.2022.104536

Kim, C. H., & Seo, J. (2019). Shallow-Depth Insertion: Peg in Shallow Hole Through Robotic In-Hand Manipulation. *IEEE Robotics and Automation Letters*, *4*(2), 383–390. https://doi.org/10.1109/LRA.2018.2890449

Koerner-Al-Rawi, J., Park, K. E., Phillips, T. K., Pickoff, M., & Tortorici, N. (2020). Robotic timber assembly. *Construction Robotics*, *4*(3), 175–185. https://doi.org/10.1007/s41693-020-00045-6

Kupczewska-Dobecka, M., Konieczko, K., & Czerczak, S. (2020). Occupational risk resulting from exposure to mineral wool when installing insulation in buildings. *International Journal of Occupational Medicine and Environmental Health*, *33*(6), 757–769. https://doi.org/10.13075/ijomeh.1896.01637

Latif, E., Bevan, R., & Woolley, T. (2019). Types of thermal insulation materials. In *Thermal Insulation Materials for Building Applications* (Vols. 1–0, pp. 5–48). ICE Publishing. https://doi.org/10.1680/timfba.63518.005

Leung, P. Y., Apolinarska, A., Tanadini, D., Gramazio, F., & Kohler, M. (2021, March 29). *Automatic Assembly of Jointed Timber Structure using Distributed Robotic Clamps*. https://doi.org/10.52842/conf.caadria.2021.1.583

Li, X., Han, S., Gül, M., & Al-Hussein, M. (2019). Automated post-3D visualization ergonomic analysis system for rapid workplace design in modular construction. *Automation in Construction*, *98*, 160–174. https://doi.org/10.1016/j.autcon.2018.11.012

Orlowski, K. (2020). Automated manufacturing for timber-based panelised wall systems. *Automation in Construction*, *109*, 102988. https://doi.org/10.1016/j.autcon.2019.102988

Spray-R | Helping prefabricators serve their customers better. (n.d.). Retrieved July 25, 2023, from Spray-R | helping prefabricators serve their customers better website: https://www.spray-r.com

Stricot-Tarboton, G. (2019). *Robotic Arm Prefab Panels: A Proof of Concept*. Retrieved from http://researcharchive.vuw.ac.nz/handle/10063/8414

Zaidi, L., Corrales, J. A., Bouzgarrou, B. C., Mezouar, Y., & Sabourin, L. (2017). Model-based strategy for grasping 3 D deformable objects using a multi-fingered robotic hand. *Robotics and Autonomous Systems*, *95*, 196–206. https://doi.org/10.1016/j.robot.2017.06.011